### REVIEW OF GROUND-BASED CMB EXPERIMENTS

A.N. LASENBY, A.W. JONES and Y. DABROWSKI Mullard Radio Astronomy Observatory, Madingley Road, Cambridge CB3 0HE, England

We present in this paper a brief review of Ground-Based Cosmic Microwave Background (CMB) experiments. We first recall the main experimental problems and adopted solutions. We then review the Tenerife experiments, giving an update together with some new results. Then results and problems from other experiments are highlighted including IAC-Bartol, Python, Saskatoon, Mobile Anisotropy Telecope (MAT) and the Owen Valley Radio Observatory (OVRO) experiments. We next move on to the future ground experiments, in particular new interferometers such as the Very Small Array (VSA), the Cosmic Background Imager (CBI) and the Degree Angular Scale Interferometer (DASI/VCA). To finish, very recent work is presented on joint likelihood analysis for estimation of cosmological parameters where both CMB results and Large Scale Structure (LSS) surveys are considered.

## 1 Experimental Problems and Solutions

## 1.1 The Contaminants

From the ground, the detection of Cosmic Microwave Background (CMB) anisotropy at the level  $\Delta T/T \sim 10^{-5}$  is a challenging problem and a wide range of experimental difficulties occur when conceiving and building an experiment. We will focus here particularly on the problem caused by the contamination of foreground sources and the solutions that have been adopted to fight against them. The anisotropic components that are of essential interest on angular scales of approximately 1/2 - 1 degree are: (i) The galactic dust emission which becomes significant at high frequencies (typically > 100 GHz). (ii) The galactic thermal (free-free) emission and non-thermal (synchrotron) radiation which are significant at frequencies lower than typically  $\sim 30$  GHz. (iii) The presence of point-like sources. (iv) The dominating source of contamination is the atmospheric emission, in particular at frequencies higher than  $\sim 10$  GHz.

## 1.2 The Solutions

A natural solution is to run the experiment at a suitable frequency so that the contaminants are kept low. There exists a window between  $\sim 10$  and  $\sim 40$  GHz where both atmospheric and galactic emissions should be lower than the typical CMB flux. For example, the Tenerife experiments are running at 10, 15 and 33 GHz and the Cambridge Cosmic Anisotropy Telescope (CAT) at 15 GHz. However, in order to reach the level of accuracy needed, spectral discrimination of foregrounds using multi-frequency data is necessary (see for example M.P. Hobson, this

volume). Concerning point (iv), three basic techniques, which are all still being used, have been developed in order to fight against the atmospheric emission problem:

The Tenerife experiments are using the *switched beam* method. In this case the telescope switches rapidly between two or more beams so that a differential measurement can be made between two different patches of the sky, allowing one to filter out the atmospheric variations.

A more modern and flexible version of the switched beam method is the *scanned beam* method (e.g. Saskatoon and Python telescopes). These systems have a single receiver in front of which a continuously moving mirror allows scanning of different patches of the sky. The motion pattern of the mirror can be re-synthesised by software. This technique provides a great flexibility regarding the angular-scale of the observations. The Saskatoon telescope has been very successful in using this system.

Finally, an alternative to differential measurement is the use of interferometric techniques. Here, the output signals from each of the baseline horns are cross-correlated so that the Fourier coefficients of the sky are measured. In this fashion one can very efficiently remove the atmospheric component in order to reconstruct a cleaned temperature map of the CMB. The Cosmic Anisotropy Telescope (CAT) operating in Cambridge has proved this method to be very successful, giving great expectations for the Very Small Array (VSA) currently being built and tested in Cambridge (jointly with Jodrell Bank) for siting in Tenerife. American projects such as the Cosmic Background Imager (CBI) and the Very Compact Array (VCA/DASI) are also planning to use this technique.

### 2 The Tenerife Experiments

[Project collaborators: Rod Davies (P.I.), Carlos Gutiérrez, Bob Watson, Rafa Rebolo]

### 2.1 Drift Scan Experiments

Due to the stability of the atmosphere and its transparency  $^1$ , the Izaña observatory of the Tenerife island is becoming very popular for cm/mm observations of the CMB (e.g. Tenerife experiments, IAC-Bartol, VSA). The three Tenerife experiments (10, 15 and 33 GHz) are each composed of two horns using the switched beam technology (angular resolution  $\sim 5$  degrees). The observations take advantage of the Earth rotation and consist of scanning a band of the sky at a constant declination. The scans have to be repeated over several days in order to achieve sufficient accuracy. See e.g. Davies et al.  $^1$  (1996) for a complete description.

The first detection at Tenerife (Dec+ $40^{\circ}$ ), which dates back to 1994 <sup>2,3</sup>, clearly reveals common structures between the three independent scans at 10, 15 and 33 GHz. The consistency between the three channels gave confidence that, for the first time, identifiable individual features in the CMB were detected <sup>4</sup>. Subsequently this was confirmed by comparing directly to the COBE DMR data <sup>5,6</sup>. Bunn, Hoffman and Silk <sup>7</sup> (1996) have applied a Wiener filter to the COBE DMR data in order to perform a prediction for the Tenerife experiments over the region  $35^{\circ} < \text{Dec} < 45^{\circ}$ . Assuming a CDM model, the COBE angular resolution has been improved in order to match the Tenerife experiments' resolution. The prediction has been observationally verified <sup>8</sup>, giving great confidence that the revealed features are indeed tracing out the seed structures present in the early universe.

### 2.2 Latest results

There is now enough data to perform a 2-D sky reconstruction  $^9$  for the 10 GHz and 15 GHz experiments (33 GHz to follow shortly). 8 separate declination scans have been performed of the full range in RA from Dec+27.5° up to Dec+45° in steps of 2.5°. This allows the reconstruction with reasonable accuracy of a strip in the sky of  $90^{\circ} \times 17.5^{\circ}$  in an area away from major point sources and the Galactic plane. The crucial aspect in obtaining accurate results is, first of

all, to allow for atmospheric correlations between the different scans. Secondly, and probably more importantly, to be aware that the maps are sensitive to unresolved discrete radio sources (typically of the Jy level in the Tenerife field) in addition to the CMB. Special analysis has been performed in order to remove these sources which have to be monitored continuously since they are variable on the time scales involved. This monitoring task is done in collaboration with M. and H. Aller (Michigan) who have a data-bank of information on these sources.

The 10 GHz 2-D map is likely to include a significant galactic contribution; however it is believed that this contribution is negligible for the 15 GHz map which reveals intrinsic Microwave Background anisotropies on 5 degrees scale. Likelihood analysis on the reconstructed 15 GHz 2-D map is in preparation and will be published shortly. Previous results <sup>3</sup> are:  $\delta T = [l(l+1)C_l/(2\pi)]^{1/2} = 34^{+15}_{-9} \mu \text{K}$  at  $l \sim 18$  (see Table 1 and Figure 1). The next step concerning the data analysis is to use the Maximum Entropy Method for frequency separation on the spherical sky, in conjunction with all sky maps such as the Haslam 408 MHz <sup>10</sup>, IRAS, Jodrell Bank (5 GHz) and COBE. The resulting frequency information will allow us to separate very accurately components such as synchrotron, free-free, dust and CMB (see M.P. Hobson, this volume), which is an exciting prospect.

# 3 Updates and Results on Various Experiments

#### 3.1 IAC-Bartol

This experiment runs with four individual channels (91, 142, 230 and 272 GHz) and is also located in Tenerife where the dry atmosphere is required for such high frequencies. This novel system is using bolometers which are coupled to a 45 cm diameter telescope. The angular resolution is approximately 2° (see elsewhere <sup>11,12,13</sup> for instrument details and preliminary results).

This switched beam system has performed observations at constant declination (Dec+40°), overlapping one of the drift scans of the Tenerife experiments. Atmospheric correlation techniques between the different channels have been applied in order to remove the strong atmospheric component present in the three lowest channels <sup>14</sup>. This atmospheric contaminant is believed to be accurately removed and the galactic synchrotron and free-free emissions are likely to be negligible at these frequencies. On the other hand, the galactic dust emission has been corrected using DIRBE and COBE DMR maps. Finally, the contamination by point-like sources was removed by multi-frequency analysis on known and unknown sources. The results obtained are  $\delta T = 113^{+66}_{-60} \mu \text{K}$  at  $l \sim 33$  and  $\delta T = 55^{+27}_{-22} \mu \text{K}$  at  $l \sim 53$  (see Table 1 and Figure 1). One can notice that the  $l \sim 33$  point is well off the expected value, however, tests show that the atmospheric component is still very high in this  $\delta T$  value. The  $l \sim 53$  point seems to be in better agreement with results from the Saskatoon or Python experiments.

# 3.2 Python

This experiment is using a single bolometer mounted on a 75cm telescope and operating at the single frequency of 90GHz with a 0.75° FWHM beam. Python is located at the Amundsen-Scott South Pole Station in Antarctica. It is performing extremely well in terms of mapping rather large regions of the sky (currently  $22^{\circ} \times 5.5^{\circ}$ ). Three seasons of observations have been analysed so far (Python I <sup>15</sup>, Python II <sup>16</sup> and Python III <sup>17</sup>). In addition to the power-spectrum results of Python III (see Table 1 and Figure 1), the combined analysis of Python I, II & III gives an estimate of the power-spectrum angular spectral index <sup>17</sup>:  $m = 0.16^{+0.2}_{-0.18}$  which is consistent with a flat-band power model (i.e. m = 0).

A point where the Python experiment differs from all the others is its single frequency measurement. All the experiments discussed here are using either widely spaced frequencies (e.g. Tenerife experiments, COBE) or closely patched bands of different frequencies (e.g. the

Table 1: Some Current Ground Based Experiments

Experiment	Frequency	Angular Scale	Site/Type	l	$\delta T$
Tenerife	$10,15,33~\mathrm{GHz}$	$\sim 5^{\circ}$	Tenerife (Switched Beam)	$18^{+9}_{-7}$	$34_{-9}^{+15}$
IAC-Bartol	91, 142, 230 and 272 GHz	$\sim 2^{\circ}$	Tenerife (Switched beam)	$33^{+24}_{-13}$ $53^{+22}_{-13}$	$113_{-60}^{+66} \\ 55_{-22}^{+27}$
Python III Python I, II & III	$90~\mathrm{GHz}$	$0.75^{\circ}$	South Pole (Scanned Beam)	$87_{-38}^{+18} \\ 170_{-50}^{+69} \\ 139_{-34}^{+99}$	$60_{-13}^{+15}  66_{-16}^{+17}  63_{-14}^{+15}$
Saskatoon	6/12 channels between 26 and 46 GHz	$0.5^{\circ} - 3^{\circ}$	Canada (Scanned Beam)	$87_{-29}^{+39}$ $166_{-43}^{+30}$ $237_{-41}^{+29}$ $286_{-38}^{+24}$ $349_{-41}^{+44}$	$49^{+8}_{-5} \\ 69^{+7}_{-6} \\ 85^{+10}_{-8} \\ 86^{+12}_{-10} \\ 69^{+19}_{-28}$
OVRO	14.56 and 32 GHz	$\sim 0.1^{\circ} - 0.4^{\circ}$	Owens Valley (Switched)	$589^{+167}_{-228}$	$56^{+8.6}_{-6.5}$

interferometers discussed in Section 4). As mentioned above, multi-frequency analysis allows identification and correction of the contaminanting component. However, near the pole, the atmospheric emission is believed to be small, while at 90 GHz the galactic dust contribution is estimated to be as small as  $\sim 2\mu K$ . On the other hand, 17 known point-like sources are present in the Python field, which are estimated to give a 2% effect in the final result. The brightest source may contribute up to 50  $\mu K$  in a single beam and ideally source removal using information from a separate telescope at the same frequency is required. Python IV and V data have already been taken and the analysis should provide power-spectrum estimations very shortly; see Kovac et al. <sup>18</sup> (1997) for details about the IV<sup>th</sup> season.

# 3.3 Saskatoon current status

The Saskatoon experiment is a scanned beam system which operates with 6 or 12 independent channels at frequencies between 26 and 46 GHz. The observations cover the North Celestial Pole with angular scales from  $0.5^{\circ}$  to  $3^{\circ}$ . The experiment has been running from 1993 to 1995 and details of the instrument as well as early results can be found elsewhere  $^{20,21}$ . To find more details about the data analysis and recent results, see for example Wollack *et al.*  $^{22}$  (1997), Netterfield *et al.*  $^{23}$  (1997) and Tegmark *et al.*  $^{24}$  (1997).

The 5 Saskatoon results (see Table 1) are crucial in constraining the position of the first Doppler peak (see Figure 1) and therefore the cosmological parameters. The overall flux calibration of the Saskatoon data was known to have a  $\pm 14\%$  error, affecting significantly estimates of Hubble's parameter  $(H_0)$  for example. However, recent work from Leitch *et al.* (private communication) who carried out joint observations of Cassiopea A and Jupiter, allows the reduction of this uncertainty. The latest calibration is now known with an estimated error of  $\sim 4\%$ .

Recent work on the foreground analysis of the Saskatoon field has been carried out by Oliveira-Costa et al.  $^{25}$  (1997). These authors found no significant contamination by point-like sources. However, they report a marginal correlation between the DIRBE 100  $\mu$ m and Saskatoon Q-Band maps which is likely to be caused by galactic free-free emission. This contamination is estimated to cause previous CMB results to be over-estimated by a factor of 1.02.

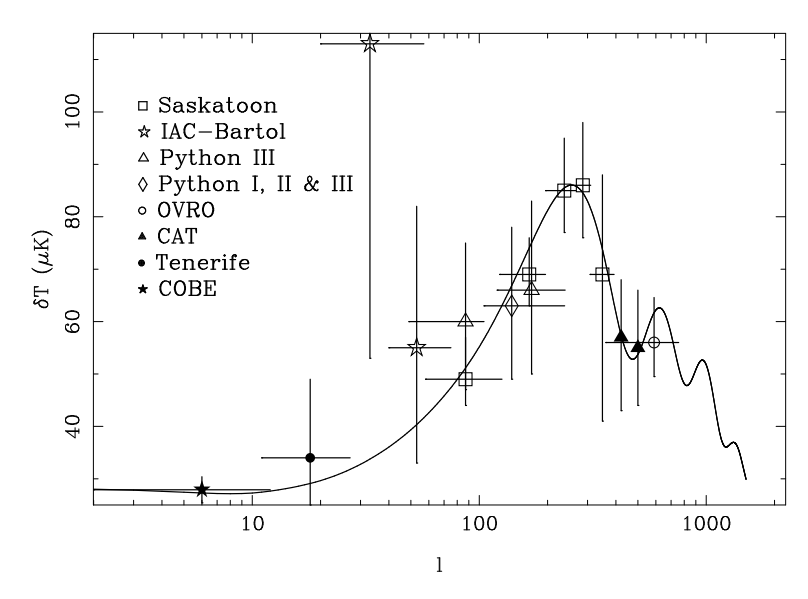


Figure 1: Plot of the CMB Power Spectrum. The data points are those presented in Table 1 and the overlaid standard CDM curve is for the parameters estimated in Section 5. the COBE data point is the 4-Year COBE DMR result (Bennett  $et\ al\ ^{19}$ . 1996) and the CAT points are given in J. Baker (this volume).

### 3.4 Mobile Anisotropy Telescope

The Mobile Anisotropy Telescope (MAT) is using the same optics and technology as Saskatoon at a high-altitude site in Chile (Atacama plateau at 5200m). This site is believed to be one of the best sites in the world for millimetre measurements and is now becoming popular for other experiments (e.g. CBI) because of its dry weather. The experiment is mounted on a mobile trailer which will be towed up to the plateau for observations and maintenance. The relevant point where MAT differs from the Saskatoon experiment is the presence of an extra channel operating at 140 GHz. This will greatly improve the resolution and should provide results well over the first Doppler peak. Data has already been taken over the last few months at 140 GHz and is currently being analysed. See the MAT www-page <sup>26</sup> for a full description of the project.

### 3.5 Owens Valley Radio Observatory

The Owens Valley Radio Observatory (OVRO) telescopes have been used since 1993 for observation of the CMB at 32 GHz and 14.5 GHz. The RING40M experiment uses the 40-meter telescope (14.5 GHz channel) while the RING5M experiment is mounted on the 5.5-meter telescope (32 GHz channel). Both experiments have an angular resolution of  $\sim 0.12^{\circ}$ . Details about these experiments can be found in Readhead *et al.* <sup>27</sup> (1989) or in Myers *et al.* <sup>28</sup> (1993) for example.

36 fields at Dec+88°, each separated by 22 arcmin, have been observed around the North Galactic Pole. Using these data, Leitch et al. <sup>29</sup> report an anomalous component of Galactic emission. Some further work on the same data (Leitch et al, private communication) gives the following estimate for the CMB component:  $\delta T = 56^{+8.6}_{-6.5} \,\mu\text{K}$  at  $l \sim 589$ . As seen on Figure 1, this new OVRO result seems to agree well with the CAT estimations and therefore helps in constraining the position of the first Doppler peak. Further details of this measurement should be available shortly.

Table 2: Future Ground Based Experiments

Experiment	Frequency	Angular Scale	Site/Type	Date
VSA	26 to 36 GHz	$0.25^{\circ} - 2^{\circ}$	Tenerife (14 element interferometer)	1999
CBI	26 to 36 GHz	$0.07^{\circ} - 0.3^{\circ}$	Chile (13 element interferometer)	1999
DASI	26 to 36 GHz	$0.25^{\circ} - 1.4^{\circ}$	South Pole (13 element interferometer)	1999

### 4 Ground Based Interferometers

As seen in Section 1.2, interferometers allow accurate removal of the atmospheric component. Therefore special ground sites are not always necessary in order to perform sensitive measurements. For example, the 3 element interferometer Cosmic Anisotropy Telescope (CAT) is currently operating in Cambridge, UK <sup>30</sup>. A full discussion of the CAT current status is given by J. Baker (this volume) and results, including the new CAT2 points, are plotted in Figure 1.

The Very Small Array (VSA) is currently being built and tested in Cambridge for siting in Tenerife and should be observing in late 1999. The 14 elements of the interferometer will operate from 26 to 36 GHz and cover angular scales from 0.25° to 2° (see Table 2). The results will consist of 9 independent bins regularly spaced from  $l \sim 150$  to  $l \sim 900$  on the Power Spectrum diagram <sup>31</sup>. This will give significant information on the second Doppler peak, while the first peak will be constrained accurately enough to estimate the total density  $\Omega$  and Hubble's constant  $H_0$ , with a 10% error. The VSA current status is discussed in this volume by M.E. Jones.

There are two other interferometer projects which will complement the work done with the VSA: The Cosmic Background Imager (CBI), to be operated from Chile by a CalTech team <sup>32</sup> and The Degree Angular Scale Interferometer <sup>33,34</sup> (DASI) – formerly Very Compact Array (VCA) – which will be operated at the South Pole (University of Chicago & CARA). They both share the same design (13 element interferometers) and the same correlator operating from 26 to 36 GHz (see Table 2). However the size of the baselines differ between CBI and DASI so that CBI will cover angular scales from 4 to 20 arcmin while DASI will cover the range between 15 arcmin and 1.4° (similar to the VSA).

All three of these interferometric experiments (VSA, CBI and DASI) should be in operation by the end of 1999.

## 5 Joining CMB and Large Scale Structures Data

As mentioned earlier, by comparing the observed CMB Power Spectrum with predictions from cosmological models one can estimate cosmological parameters  $^{3,35,36}$ . In an independent manner, similar predictions can be achieved by comparing Large Scale Structure (LSS) surveys with cosmological models  $^{37,38,39}$ . Recently, Webster et al.  $^{40}$  propose to use full likelihood calculations in order to join CMB and LSS predictions. They use results from various independent CMB experiments together with the IRAS 1.2 Jy galaxy redshift survey and parametrise a set of spatially flat models. Because the CMB and LSS predictions are degenerate with respect to different parameters (roughly:  $\Omega_m \text{vs } \Omega_\Lambda$  for CMB;  $H_0$  and  $\Omega_m \text{vs } b_{\text{iras}}$  for LSS), the combined data likelihood analysis allows the authors to break these degeneracies, giving remarkable parameter predictions. We note that  $\Omega_m$  is the overall matter density. A preliminary result of the joint likelihood calculations is given in Figure 2 showing a well-defined peak for  $\Omega_m$  and  $H_0$ , together with the corresponding optimal value for the IRAS light-to-mass bias ( $b_{\text{iras}}$ ).

The preliminary best fit results from the two data sets joint analysis on all the free parameters

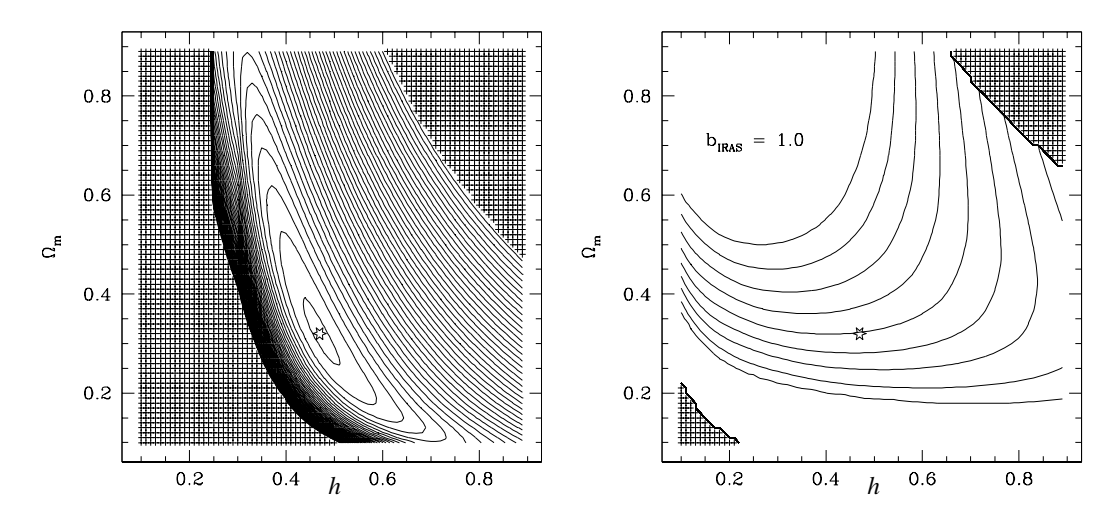


Figure 2: Plots on the  $(\Omega_m, h)$  plane, where  $h = H_0/100 \text{ km s}^{-1}$ . Left: Likelihood contours defining the optimum values for  $(\Omega_m, h)$ . Right:  $b_{\text{iras}}$  contours with corresponding optimal value for  $b_{\text{iras}} = 1$ .

are <sup>40</sup> (marginalised error bars for 95% confidence):  $\Omega_m = 0.32 \pm 0.08$ ,  $\Omega_b = 0.061 \pm 0.013$ ,  $H_0 = 47 \pm 6$  km s<sup>-1</sup> Mpc<sup>-1</sup>,  $b_{\rm iras} = 1.04 \pm 0.06$  and  $\sigma_8 = 0.78 \pm 0.1$ , where  $\Omega_b$  is the baryonic density and  $\sigma_8$  is the variance measured in a 8 Mpc radius sphere.

#### 6 Conclusion

Ground-based CMB experiments are already providing significant constraints on cosmological models, particularly the interferometers and future ground-based experiments, will sharpen these up considerably. Although full-sky high resolution satellite experiments like Planck Surveyor will eventually provide definite answers for the CMB, the ability of ground-based experiments to go deep on selected patches, and the controllability and accessibility of such experiments, mean that they will have a very important role for some years to come.

### References

- 1. R.D. Davies, C.M. Gutiérrez, J. Hopkins, S.J. Melhuish, R.A. Watson, R.J. Hoyland, R. Rebolo, A.N. Lasenby and S. Hancock, MNRAS **278**, 883 (1996).
- 2. S. Hancock, R.D. Davies, A.N. Lasenby, C.M.G. Delacruz, R.A. Watson, R. Rebolo and J.E. Beckman, Nature **367**, 333 (1994).
- 3. S. Hancock, C.M. Gutiérrez, R.D. Davies, A.N. Lasenby, G. Rocha, R. Rebolo, R.A. Watson and M. Tegmark, MNRAS **289**, 505 (1997).
- 4. A.N. Lasenby, S. Hancock, R.D. Davies, C.M.G. Delacruz, R.A. Watson and R. Rebolo, A.L.& COMM 32, 191 (1995)
- C.H. Lineweaver, S. Hancock, G.F. Smoot, A.N. Lasenby, R.D. Davies, A.J. Banday, C.M.G. Delacruz, R.A. Watson and R. Rebolo, ApJ 448, 482 (1995).
- S. Hancock, A.N. Lasenby, C.M.G Delacruz, R.D. Davies, R.A. Watson and R. Rebolo, A.L.& COMM 32, 201 (1995).
- 7. E.F. Bunn, Y. Hoffman and J. Silk, ApJ 464, 1 (1996).
- 8. C.M. Gutierrez, S. Hancock, R.D. Davies, R. Rebolo, R.A. Watson, R.J. Hoyland, A.N. Lasenby and A.W. Jones, ApJ 480, L83 (1997).
- 9. A.W. Jones, S. Hancock, A.N. Lasenby, R.D. Davies, C.M. Gutiérrez, G. Rocha, R.A. Watson and R. Rebolo, MNRAS **294**, 582 (1998).
- 10. C.G.T. Haslam, H. Stoffel, C.J. Salter and W.E. Wilson, A&A Supp. S. 47, 1 (1982).

- 11. L. Piccirillo, Rev. Sci. Instr. **62**, 1293 (1991).
- 12. L. Piccirillo and P. Calisse, ApJ 411, 529 (1993).
- 13. L. Piccirillo et al., ApJ **475**, L77 (1997).
- 14. B. Femenia, R. Rebolo, C.M. Gutiérrez, M. Limon and L. Piccirillo, ApJ, in press, astro-ph/9711225 (1998).
- M. Dragovan, J.E. Ruhl, G. Novak, S.R. Platt, B. Crone, R. Pernic and J.B. Peterson, ApJ 427, L67 (1994).
- 16. J.E. Ruhl, M. Dragovan, S.R. Platt, J. Kovac and G. Novak, ApJ 453, L1 (1995).
- 17. S.R. Platt, J. Kovac, M. Dragovan, J.B. Peterson and J.E. Ruhl, ApJ 475, L1 (1997).
- 18. J. Kovac, M. Dragovan and D.A. Schleuning, BAAS 191, 112 (1997).
- 19. C.L. Bennett, A. Banday, K.M. Górski, G. Hinshaw, P. Jackson, P. Keegstra, A. Kogut, G.F. Smoot, D.T. Wilkinson and E.L. Wright, ApJ **464**, L1 (1996).
- E.J. Wollack, N.C. Jaroski, C.B. Netterfield, L.A. Page and D. Wilkinson, ApJ 419, L49 (1993).
- 21. E.J. Wollack, M.J. Devlin, N.C. Jaroski, C.B. Netterfield, L. Page and D. Wilkinson, Tech. Rep. Princ. Univ, 01/1996 (1996).
- 22. E.J. Wollack, M.J. Devlin, N.C. Jaroski, C.B. Netterfield, L. Page and D. Wilkinson, ApJ 476, 440 (1997).
- 23. C.B. Netterfield, M.J. Devlin, N.C. Jaroski, L. Page and E.J. Wollack, ApJ 474, 47 (1997).
- 24. M. Tegmark, A. Oliveira-Costa, M.J. Devlin, C.B. Netterfield, L. Page and E.J Wollack, ApJ 474, L77 (1997).
- A. Oliveira-Costa, A. Kogut, M.J. Devlin, C.B. Netterfield, L. Page and E.J. Wollack, Ap.J 482, L17 (1997).
- 26. T. Herbig, http://tyger.princeton.edu/~th/mat/mat.html
- 27. A.C.S. Readhead, C.R. Lawrence, S.T. Myers, W.L.W. Sargent, H.E. Hardebeck and A.T. Moffet, ApJ 346, 566 (1989).
- 28. S.T. Myers, A.C.S. Readhead and C.R. Lawrence, ApJ 405, 8 (1993).
- 29. E.M. Leitch, A.C.S. Readhead, T.J. Pearson and S.T Myers, ApJ 486, L23 (1997).
- 30. P.F. Scott, R. Saunders, G. Pooley, C. Osullivan, A.N. Lasenby, M. Jones, M.P. Hobson, P.J. Duffettsmith and J. Baker, ApJ **461**, L1 (1996).
- 31. M.E. Jones, in *Microwave Background Anisotropies (1996)*, F.R. Bouchet, R. Gispert, B. Guiderdoni and J. Tran Thanh Van, editors, Editions Frontières, Paris (1997).
- 32. T.J. Pearson, http://astro.caltech.edu/~tjp/CBI/
- 33. M. White, J.E. Carlstrom and M. Dragovan, Submitted to ApJ, astro-ph/9712195 (1997).
- 34. A.A. Stark, J.E. Carlstrom, F.P. Israel, K.M. Menten, J.B. Peterson, T.G. Phillips, G. Sironi and C.K. Walker, pre-print, astro-ph/9802326 (1998).
- 35. S. Hancock, G. Rocha, A.N. Lasenby and C.M. Gutiérrez, MNRAS 294, L1 (1998).
- 36. C.H Lineweaver, D. Barbosa, A. Blanchard and J.G. Bartlett, A&A 322, 365 (1997).
- 37. J.A. Willick, M.A. Strauss, A. Dekel and T. Kolatt, ApJ 486, 629 (1997).
- 38. K.B. Fisher and A. Nusser, MNRAS **279**, L1 (1996).
- 39. A.F. Heavens and A.N. Taylor, MNRAS **275**, 483 (1995).
- 40. M. Webster, M.P. Hobson, A.N. Lasenby, O. Lahav and G. Rocha, ApJ.L, in press, astro-ph/9802109 (1998).